Surface Science 84 (1979) 355–374

$Si–SiO_2$ INTERFACE CHARACTERIZATION BY ESCA

Akitoshi ISHIZAKA, Seiichi IWATA and Yoshiaki KAMIGAKI
Central Research Laboratory, Hitachi, Ltd., Kokubunji, Tokyo, Japan

Received 17 July 1978; manuscript received in final form 14 February 1979

The concentration profiles of oxide films on Si have been studied by using ESCA and ellipsometry. To avoid artifacts from ion milling or chemical thinning, our analyses have been performed on grown oxides up to 5 nm thick on Si. The accurate values of the escape depths obtained from ESCA and the ellipsometric measurements in this study were used to analyze the intensity data for Si_{2p} and O_{1s} photoelectrons. Furthermore, the chemical states of Si atoms have been analyzed. The oxide films were found to be composed mostly of stoichiometric SiO_2 with a very thin (about 0.3 nm) layer of SiO at the $Si–SiO_2$ interface, although the composition of oxide films appeared to be Si-rich in appearance for thicknesses less than about 3 nm.

1. Introduction

The characterization of the $Si–SiO_2$ interface is important for the Si semiconductor device development, from both fundamental and practical points of view. Many studies on the $Si–SiO_2$ interface have been made by using electron spectroscopy for chemical analysis (ESCA) [1–5], Auger electron spectroscopy (AES) [6–8], secondary ion mass spectroscopy (SIMS) [9,10], ion scattering spectroscopy (ISS) [11], optical reflectance [12,13] and transmission electron microscopy [14,15]. In these studies, it has been reported that a non-stoichiometric layer existed at the $Si–SiO_2$ interface. However, there were significant differences among these results. Spicer et al. [6,7] proposed that a mixture phase, composed of Si and SiO_2, existed at the transition region (~4 nm thick). Raider et al. [5] proposed that the oxide film in the transition region (~1 nm thick) changed continuously as SiO_x. Grunthaner et al. [4] proposed that the oxidation state of the Si atoms in the transition region (0.3–0.7 nm) changed from 0 to +4. It is the purpose of this study to clarify the composition and the chemical state of the oxide film near the $Si–SiO_2$ interface.

Quantitative analysis by ESCA seemed to be easier than that by AES, because the peak-to-peak height of the differentiated curves in the AES spectra is generally measured for Auger electron intensity. The SIMS, ISS and optical reflectance methods are only semi-quantitative. ESCA was therefore used for this study.

One way to determine the concentration profile in the oxide film is to measure

the composition by ESCA after thinning the oxide by ion or chemical etching as Grunthaner [4] did. However, this method was not used in this study because ion or chemical etching may cause non-uniformity of thickness or change in the chemical state of the oxide film being tested, thus preventing quantitative analysis. Instead, the concentration profile was obtained from the composition and chemical state analyses of very thin oxide films up to 5 nm thick, in which the interface compositions were assumed to be the same.

This study was conducted in two stages. First, the mean escape depth (λ) of emitted photoelectrons was determined, because there were several different reported values of λ for the $Si-SiO_2$ system [2,16–20], and it was not known which one should be used in this study. This value is essential for an accurate quantitative evaluation of the photoelectron intensity data in ESCA measurements. Secondly, the $Si-SiO_2$ interface was characterized in three steps. The first step was the determination of the apparent composition (see section 3.3) of the oxide film using the photoelectron intensity data and the experimentally determined λ values. The next dealt with the chemical state determination from the peak positions in the photoelectron spectra, and the last step dealt with the determination of the true concentration profile in the oxide film on Si using the previously obtained results.

2. Experimental method

The value of the mean escape depth, necessary for quantitative composition anlysis, was first determined from the relationship between the oxide film thickness measured by ellipsometry and the photoelectron intensity measured by ESCA. The composition and the chemical state were then determined from the intensity data and the peak positions in the photoelectron spectra from the ESCA measurements.

2.1. Sample preparation

The samples were very thin oxide films (1–5 nm thick) grown on Si single crystals by thermal oxidation. The Si wafers used in this work were boron (B)-doped, mechano-chemically mirror-polished, (100) oriented, and they had an electrical resistivity of 2Ω cm.

The samples were prepared in a clean (class 100) room. They were cleaned by the following processes. First they were etched chemically in 1 : 20 $HF-HNO_3$, to remove the damaged layer created by polishing, then boiled in 3 : 1 : 20 $H_2O_2-HCl-H_2O$, further boiled in 1 : 1 : 2 $H_2O_2-NH_4OH-H_2O$, next dipped in 2% HF solution to remove the oxide film formed during these chemical treatments, and finally rinsed in deionized water.

The samples were then put into a resistance-heated 3-zone furnace within 1 min after chemical cleaning. Two samples were oxidized at the same time, one for ESCA and another for ellipsometric measurements. The oxidation temparature was con-

trolled to within ±1°C in the range of 550 to 900°C. The oxidation atmosphere was an O_2/N_2 mixture, with the ratio being controlled by a mass flow meter, and the desired partial pressure of O_2 was $0.5 \times 10^2 \sim 4 \times 10^2$ Pa. After the desired oxidation time (8–240 min), the samples were rapidly removed from the furnace.

2.2. Ellipsometric measurement

The oxide film thickness, required for determining the mean escape depth for emitted photoelectrons, was measured by using a split beam type ellipsometer (Mizojiri Kogaku, Ltd.).

The wavelength of the light used was 546.1 nm, and the angle of incidence was 70.00°. The refractive indices of Si and SiO_2 were $4.08–0.028i$ and 1.47, respectively, determined from the relationship between the analyzer and polarizer angles for the oxide films of various thicknesses (1–100 nm). These index values also agreed with the reported values [21–23]. Data analyses for obtaining oxide film thicknesses were then carried out by using McCrackin's computer program [24].

The ellipsometric measurements were carried out in air. They were completed within 15 min after the oxidation was completed, in order to minimize the changes in the sample condition due to adsorption or further oxidation. In these measurements, the relative thickness error defined as the ratio of the standard deviation to average value, was within 1%.

2.3. ESCA measurement

The photoelectron spectra were obtained by using a Hitachi E-507 ESCA, which had a cylindrical mirror type analyzer, a multi-channel analyzer (512 channels) and an oil free vacuum. MgKα (1253.6 eV) radiation was used to excite the photoelectrons from the sample. The acceleration voltage and the emission current used for producing the X-rays were 10 kV and 50 mA, respectively. The samples (10×10 mm^2 in area) were mounted on a Cu sample holder by means of a Ag conductive paste after removing the oxide films on the back-surface of Si, and the sample holder was at the same potential as the spectrometer. The sample was mounted on a sample probe about 5 min after the oxidation was completed and it was inserted into the analyzer chamber of the ESCA instrument which was kept at a vacuum of 1×10^{-4} Pa after 10 min evacuation in the preparation chamber.

The intensities and peak positions of Si_{2p} and O_{1s} spectra were measured. The photoelectron intensity was defined as the area of the peak. The relative error, defined as the ratio of the standard deviation to the average value, was 2.3% for the ratio of the O_{1s} intensity ($I_{O_{1s}}$) to the Si_{2p} intensity ($I_{Si_{2p}}$) from SiO_2. The peak position could be determined to within ±0.1 eV of the electron energy.

2.4. Analysis of photoelectron intensity data

The photoelectron intensity data for Si_{2p} and O_{1s} spectra were analyzed to determine the various λ values and the composition of the oxide film on Si.

The intensity of the Si_{2p} photoelectrons emitted from the oxide film ($I^{oxide}_{Si_{2p}}$), that from the Si substrate ($I^{Si}_{Si_{2p}}$) and that of the O_{1s} from the oxide film ($I^{oxide}_{O_{1s}}$) can be written as [16]

$$I^{oxide}_{Si_{2p}} = KF\,\sigma^{oxide}_{Si_{2p}}\, n^{oxide}_{Si}\, \lambda^{oxide}_{Si_{2p}}\, [1 - \exp(-1.35 d_{ESCA}/\lambda^{oxide}_{Si_{2p}})], \tag{1}$$

$$I^{Si}_{Si_{2p}} = KF\,\sigma^{Si}_{Si_{2p}}\, n^{Si}_{Si}\, \lambda^{Si}_{Si_{2p}} \exp(-1.35 d_{ESCA}/\lambda^{oxide}_{Si_{2p}}), \tag{2}$$

$$I^{oxide}_{O_{1s}} = KF\,\sigma^{oxide}_{O_{1s}}\, n^{oxide}_{O}\, \lambda^{oxide}_{O_{1s}}\, [1 - \exp(-1.35 d_{ESCA}/\lambda^{oxide}_{O_{1s}})], \tag{3}$$

where K is the instrumental factor, which is constant for energies of 30 to 1500 eV for our ESCA, F is the X-ray intensity, σ^{j}_{lm} is the photoionization cross section for the m level electrons of the l atoms in the j material, n^{j}_{i} is the number of the i atoms in a unit volume of the j material, λ^{j}_{lm} is the mean escape depth for the emitted photoelectrons from the m level of the l atoms in the j material, defined as the distance at which the escape probability of the excited electrons is 1/e of their intensity at the surface, d_{ESCA} is the oxide film thickness obtained by ESCA, and the value 1.35 is equal to $1/\cos(42.5°)$ in which 42.5° is the electron acceptance angle of the analyzer in relation to the line perpendicular to the sample surface. These are three fundamental equations for obtaining the mean escape depth values (λ) and for the compositional analysis of the oxide film on Si.

The λ values were obtained by using two methods. The λ values for Si^{oxide}_{2p} and Si^{Si}_{2p} were obtained by the method proposed by Carlson [25]. This method can be used when the peaks from the oxide film and the substrate are associated with photoelectrons from the same level. Eq. (4) can be obtained by dividing eq. (1) by eq. (2) as [2,25]

$$\frac{I^{oxide}_{Si_{2p}}}{I^{Si}_{Si_{2p}}} = \frac{\sigma^{oxide}_{Si_{2p}}\, n^{oxide}_{Si}\, \lambda^{oxide}_{Si_{2p}}}{\sigma^{Si}_{Si_{2p}}\, n^{Si}_{Si}\, \lambda^{Si}_{Si_{2p}}} \left[\exp\left(\frac{1.35 d_{ESCA}}{\lambda^{oxide}_{Si_{2p}}}\right) - 1\right]. \tag{4}$$

Then, by making use of this equation, the $\lambda^{oxide}_{Si_{2p}}$ and $\lambda^{Si}_{Si_{2p}}$ values can be determined from the data for $I^{oxide}_{Si_{2p}}/I^{Si}_{Si_{2p}}$, obtained by ESCA, and that for the oxide film thickness obtained by ellipsometry.

On the other hand, the $\lambda^{oxide}_{O_{1s}}$ value was determined from $I^{oxide}_{O_{1s}}$ and the oxide film thickness data by using eq. (3). Since F in eq. (3) changed by about ±5% with each measurement, F was obtained from the Si_{2p} intensity value (equal to $I^{Si}_{Si_{2p}} + I^{oxide}_{Si_{2p}}$). By combining eqs. (1) and (2), F can be written as

$$F = (I^{Si}_{Si_{2p}} + I^{oxide}_{Si_{2p}})\, [\sigma^{oxide}_{Si_{2p}}\, n^{oxide}_{Si}\, \lambda^{oxide}_{Si_{2p}} + (\sigma^{Si}_{Si_{2p}}\, n^{Si}_{Si}\, \lambda^{Si}_{Si_{2p}} - \sigma^{oxide}_{Si_{2p}}\, n^{oxide}_{Si}\, \lambda^{oxide}_{Si_{2p}}) \times \exp(-1.35 d_{ESCA}/\lambda^{oxide}_{Si_{2p}})]^{-1}, \tag{5}$$

These λ values, $\lambda^{oxide}_{Si_{2p}}$, $\lambda^{Si}_{Si_{2p}}$ and $\lambda^{oxide}_{O_{1s}}$, were used for the compositional analysis. The composition of the oxide film was determined from the photoelectron

intensity ratio, $I_{O_{1s}}^{oxide}/I_{Si_{2p}}^{oxide}$, by dividing eq. (3) by eq. (1) as

$$\frac{I_{O_{1s}}^{oxide}}{I_{Si_{2p}}^{oxide}} = \frac{\sigma_{O_{1s}}^{oxide} n_O^{oxide} \lambda_{O_{1s}}^{oxide} [1 - \exp(-1.35 d_{ESCA}/\lambda_{O_{1s}}^{oxide})]}{\sigma_{Si_{2p}}^{oxide} n_{Si}^{oxide} \lambda_{Si_{2p}}^{oxide} [1 - \exp(-1.35 d_{ESCA}/\lambda_{Si_{2p}}^{oxide})]}, \quad (6)$$

The quantity, $n_O^{oxide}/n_{Si}^{oxide}$, was defined as "the apparent composition", and could be obtained from eq. (6) by assuming a constant composition in the oxide film (see section 3.4).

The concentration profile was obtained by comparing the experimental value of $I_{O_{1s}}^{oxide}/I_{Si_{2p}}^{oxide}$ with the calculated one for various concentration profiles assumed on the basis of the chemical state analysis. The following assumptions were made for the calculation of $I_{O_{1s}}^{oxide}/I_{Si_{2p}}^{oxide}$.

(1) The concentration profile near the Si–SiO_2 interface is the same for all oxide film thicknesses.

(2) The film is composed of two layers, namely, SiO_2 of thickness d_2 and an intermediate phase, SiO, of constant thickness d_1.

3. Results and discussion

3.1. ESCA peaks

Typical examples of spectra for Si_{2p} and O_{1s} photoelectrons obtained in this study are shown in fig. 1. The Si_{2p} spectrum is made up of the Si_{2p}^{Si} and Si_{2p}^{oxide} peaks, the former being higher in kinetic energy than the latter. A careful analysis of the spectra shows that there are actually three peaks, two of which are associated with oxidized Si, i.e., Si_{2p}^{oxide} is due to the photoelectrons from SiO_2 and those from another phase (probably SiO). This will be explained in detail in section 3.4.

The intensities of the Si_{2p}^{oxide} and O_{1s}^{oxide} peaks increase and that of Si_{2p}^{Si} decreases, as oxidation proceeds. The position of the Si_{2p}^{Si} peak is almost constant at 1150.8(4) eV in kinetic energy for all samples within a standard deviation of 0.1(6) eV. However, the position of the Si_{2p}^{oxide} peak moves from 1147.7 to 1146.1 eV, and that of the O_{1s}^{oxide} peak from 717.9 to 716.5 eV with the increase in oxide film thickness.

The intensity of the Si_{2p}^{oxide} peak was defined in this study as the total intensity of the Si_{2p} spectrum minus the intensity of the Si_{2p}^{Si} peak. The Si_{2p}^{Si} peak shape was assumed to be similar to that of a freshly etched Si crystal with a negligible contribution from the peak associated with SiO_2. For such a sample, a small O_{1s} peak, which was probably due to physical adsorption or chemisorption, was observed. This O_{1s} peak intensity for a freshly etched sample corresponds to an oxide thickness of less than 0.1 nm thick [see eq. (12)].

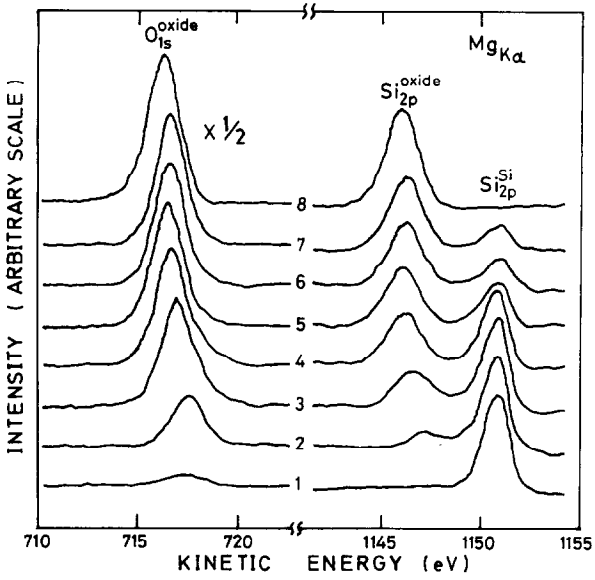

Fig. 1. Typical examples of O_{1s} and Si_{2p} photoelectron spectra for various oxide thicknesses (by ellipsometry): (1) 0.60 nm (freshly etched Si); (2) 1.00 nm; (3) 1.50 nm; (4) 2.14 nm; (5) 2.99 nm; (6) 4.03 nm; (7) 4.90 nm; (8) 200 nm.

3.2. Determination of mean escape depths

The mean escape depth values, λ_{2p}^{oxide}, $\lambda_{Si_{2p}}^{Si}$ and $\lambda_{O_{1s}}^{oxide}$, are determined in this section under the assumptions that the oxide film is of uniform composition and that the same λ can be used for oxide films of different thicknesses.

First, the $\lambda_{Si_{2p}}^{oxide}$ and $\lambda_{Si_{2p}}^{Si}$ values were determined by using eq. (4). The relationship between $I_{Si_{2p}}^{oxide}/I_{Si_{2p}}^{Si}$, measured by ESCA, and the oxide film thickness measured by ellipsometry, $d_{ellipso}$, is shown in fig. 2. In eq. (4), the oxide film thickness is not $d_{ellipso}$ but d_{ESCA}. It will be assumed here that

$$d_{ESCA} = d_{ellipso} - C, \tag{7}$$

where C is a constant value. The difference in the value of the thickness as measured by ESCA and by ellipsometry seems to be due to the difference in the definition of the Si–SiO_2 interface position for these two methods as reported by Chang [8], and/or the degree of influence of adsorption, because the ESCA measurement is made in vacuum and the ellipsometrial measurement in air.

Eq. (4) is rewritten as

$$I_{Si_{2p}}^{oxide}/I_{Si_{2p}}^{Si} = A\{\exp[B(d_{ellipso} - C)] - 1\}\ , \tag{8}$$

by substituting eq. (7) into eq. (4), where

$$A = \sigma_{Si_{2p}}^{oxide} n_{Si}^{oxide} \lambda_{Si_{2p}}^{oxide} / \sigma_{Si_{2p}}^{Si} n_{Si}^{Si} \lambda_{Si_{2p}}^{Si}, \quad (9)$$

$$B = 1.35/\lambda_{Si_{2p}}^{oxide}. \quad (10)$$

The values of A, B and C were determined by the method of least squares by using the data for oxide films of 1–5 nm thick. The values obtained were $A = 0.779 \pm 0.019$, $B = 0.387 \pm 0.001$ nm^{-1} and $C = 0.04 \pm 0.02$ nm. The value of $\lambda_{Si_{2p}}^{oxide}$ obtained from eq. (10) was 3.49 ± 0.01 nm. The value of $\lambda_{Si_{2p}}^{Si}$ was next obtained from eq. (9). If it is assumed that the oxide is almost all SiO_2, the ratio $(n_{Si}^{oxide}/n_{Si}^{Si})$ in eq. (9) is rewritten as

$$n_{Si}^{oxide}/n_{Si}^{Si} = (\rho_{SiO_2}/M_{SiO_2})(\rho_{Si}/M_{Si})^{-1}, \quad (11)$$

where ρ is the density [26–28], being 2.42 Mg/m^3 for Si and 2.21 Mg/m^3 for SiO_2; M is the molecular weight, being 28.1 g for Si and 60.1 g for SiO_2. It can also be assumed that $\sigma_{Si_{2p}}^{oxide}$ (or $\sigma_{Si_{2p}}^{SiO_2}$) is equal to $\sigma_{Si_{2p}}^{Si}$ [29,30]. As a result, the value of $\lambda_{Si_{2p}}^{Si}$ obtained by substituting just these values into eq. (9) was 1.91 ± 0.05 nm (there is an uncertainty in this value, because n_{Si}^{oxide} is not exactly $n_{Si}^{SiO_2}$; the actual value will be determined in the Appendix).

Next, the value of $\lambda_{O_{1s}}^{oxide}$ was determined by using eq. (3), which can be rewritten as

$$1 - I_{O_{1s}}^{oxide}/I_{O_{1s}}^{oxide}(d = \infty) = \exp[(C' - d_{ellipso})D], \quad (12)$$

where

$$I_{O_{1s}}^{oxide}(d = \infty) = F \sigma_{O_{1s}}^{oxide} n_{O}^{oxide} \lambda_{O_{1s}}^{oxide},$$

$$D = 1.35/\lambda_{O_{1s}}^{oxide}.$$

The relationship between $\log[1 - I_{O_{1s}}^{oxide}/I_{O_{1s}}^{oxide}(d = \infty)]$ and $d_{ellipso}$ is shown in fig. 3. The value of the intensity $I_{O_{1s}}^{oxide}(d = 200$ nm) for the 200 nm thick oxide film was used for $I_{O_{1s}}^{oxide}(d = \infty)$, because $\lambda_{O_{1s}}^{oxide}$ is much smaller than 200 nm [see eq. (3)]. The values of $\lambda_{O_{1s}}^{oxide}$ and C' were determined by the method of least squares, and the obtained values were 1.68 ± 0.03 nm and 0.28 ± 0.01 nm for $\lambda_{O_{1s}}^{oxide}$ and C', respectively. The C' value obtained is different from C in eq. (8) ($C = 0.04$ nm). This means that the oxide thickness d_{ESCA} obtained from the Si_{2p}^{oxide} photoelectron intensity (d_{ESCA}^{Si}) is not the same as that from the O_{1s}^{oxide} intensity (d_{ESCA}^{O}). The value of C' is roughly equal to the thickness of the transition layer between Si and SiO_2 as will be shown in sections 3.4 and 3.5.

These λ values obtained agree with some, and disagree with other values which have been reported by other researchers. The present value for $\lambda_{O_{1s}}^{oxide}$ roughly agrees with the one reported by Flitsch et al. for $\lambda_{O_{1s}}^{SiO_2}$ (1.8 nm) [2].

Next, the present value for $\lambda_{Si_{2p}}^{oxide}$ (3.49 nm) is considerably larger than the theoretical value of Penn [17,18] (1.7 nm) and the experimental value of Flitsch et al.

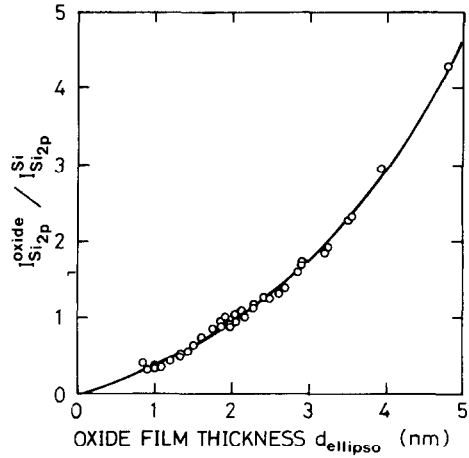

Fig. 2. Relationship between $I^{oxide}_{Si_{2p}}/I^{Si}_{Si_{2p}}$ and oxide film thickness, $d_{ellipso}$, by ellipsometry. The solid curve was obtained by the method of least squares. The $\lambda^{oxide}_{Si_{2p}}$ and $\lambda^{Si}_{Si_{2p}}$ values were determined from this relationship.

[2] (2.5 nm). However, our value is roughly equal to those of Leonhardt et al. [20] (3.8 nm at 1145 eV in kinetic energy), Klasson et al. [16] (4.8 nm at 1609 eV in kinetic energy) and Grunthaner [19] (~4.0 nm at 1380 eV in kinetic energy). Although the low value of $\lambda^{SiO_2}_{Si_{2p}}$ obtained by Flitsch et al. could not be explained, the present value of 3.49 nm was used in the compositional analysis since it was obtained from a careful analysis of the data from ESCA and ellipsometry measurements, and it was in fair agreement with three other reported values.

It is interesting to note that $\lambda^{SiO_2}_{Si_{2p}}$ is quite different from $\lambda^{Si}_{Si_{2p}}$, although λ is usually considered to depend mainly on the kinetic energy of the electrons, and other researchers [2,16] have reported that $\lambda^{Si}_{Si_{2p}}$ was nearly equal to $\lambda^{SiO_2}_{Si_{2p}}$. Since the energies of the emitted photoelectrons from the oxide film and Si are almost equal, this means that λ considerably depends on the material in which the electrons pass, which is quite reasonable. A similar phenomenon was reported for the WO_3/W system by Carlson [25], where $\lambda^{WO_3}_{W_{4f}}$ (1440 eV) was 2.63 nm and $\lambda^{W}_{W_{4f}}$ (1445 eV) was 1.28 nm.

The λ value is essential for analyzing the photoelectron intensity data. These λ values just obtained were used for the composition analysis of oxide films on Si described in the next section.

3.3. Apparent composition of thin oxide films on Si

The compositions of oxide films on Si were determined from the ratios of the O^{oxide}_{1s} to Si^{oxide}_{2p} peak intensities.

The relationship between the intensity ratio ($I^{oxide}_{O_{1s}}/I^{oxide}_{Si_{2p}}$) and the oxide film thickness was first obtained as shown in fig. 4. The solid curve in fig. 4 represents

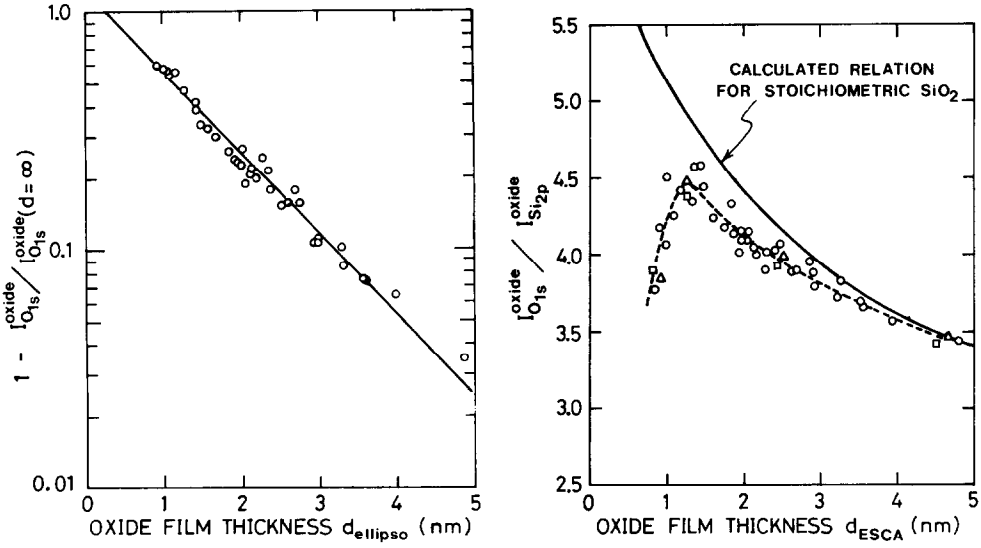

Fig. 3. Relationship between $[1 - I^{oxide}_{O_{1s}}/I^{oxide}_{O_{1s}}(d = \infty)]$ and $d_{ellipso}$. The solid line was obtained by the method of least squares. The $\lambda^{oxide}_{O_{1s}}$ value was determined from this relationship.

Fig. 4. Relationship between $I^{oxide}_{O_{1s}}/I^{oxide}_{Si_{2p}}$ and oxide film thickness, d_{ESCA}, by ESCA. The solid curve represents the calculated relation for stoichiometric SiO_2. (△) Before heating; (□) after heating at 300°C for 1 h in ESCA to remove the adsorption layer.

the calculated relation based on eq. (6) for stoichiometric SiO_2 and this was obtained as follows. When the oxide film is much thicker than λ, $I^{oxide}_{O_{1s}}/I^{oxide}_{Si_{2p}}$ is almost equal to

$$(\sigma^{SiO_2}_{O_{1s}} n^{SiO_2}_{O} \lambda^{SiO_2}_{O_{1s}})/(\sigma^{SiO_2}_{Si_{2p}} n^{SiO_2}_{Si} \lambda^{SiO_2}_{Si_{2p}}),$$

and this value was 2.96 for a 200 nm thick oxide film. Then, eq. (6) can be rewritten as eq. (13) by substituting this value and the λ values:

$$\frac{I^{SiO_2}_{O_{1s}}}{I^{SiO_2}_{Si_{2p}}} = 2.96 \frac{1 - \exp(-0.804 d_{ESCA})}{1 - \exp(-0.387 d_{ESCA})}. \tag{13}$$

The solid curve decreases with increasing SiO_2 thickness and this can be explained by the difference in the values of $\lambda^{SiO_2}_{O_{1s}}$ and $\lambda^{SiO_2}_{Si_{2p}}$. In fig. 4, the experimental value of the oxide film thickness was determined by rewriting eq. (4) as

$$d_{ESCA} = 2.59 \ln(1.28 I^{oxide}_{Si_{2p}}/I^{Si}_{Si_{2p}} + 1). \tag{14}$$

The d_{ESCA} just obtained had a good linear relation with $d_{ellipso}$, although this dif-

fered from Raider's result [5], where d_{ESCA} deviated from $d_{ellipso}$ for oxide films less than ~2 nm thick.

In fig. 4, the effect of adsorption on the $I^{oxide}_{O_{1s}}/I^{oxide}_{Si_{2p}}$ ratio was also studied. Triangle marks represent the data measured at room temperature and square marks represent those measured at 300°C for 1 h in ESCA to remove the adsorption layer on SiO_2, which probably contains C, H and O atoms. However, there is no assurance that the adsorption layer can be completely removed by heating at 300°C, and the effect of adsorption on the ratio $I^{oxide}_{O_{1s}}/I^{oxide}_{Si_{2p}}$ is not known. The following consideration was therefore carried out. The change of the $I^{oxide}_{O_{1s}}/I^{oxide}_{Si_{2p}}$ ratio by adsorption, Δ, is expressed as

$$\Delta = \frac{I^{ad}_{O_{1s}} + I^{oxide}_{O_{1s}} \exp(-d_{ad}/\lambda^{ad}_{O_{1s}})}{I^{oxide}_{Si_{2p}} \exp(-d_{ad}/\lambda^{ad}_{Si_{2p}})} - \frac{I^{oxide}_{O_{1s}}}{I^{oxide}_{Si_{2p}}}, \tag{15}$$

where d_{ad} is the adsorption layer thickness multiplied by 1.35. As

$$I^{ad}_{O_{1s}} = \sigma^{ad}_{O_{1s}} n^{ad}_{O} \lambda^{ad}_{O_{1s}} [1 - \exp(-d_{ad}/\lambda^{ad}_{O_{1s}})] = K[1 - \exp(-d_{ad}/\lambda^{ad}_{O_{1s}})], \tag{16}$$

where

$$K = \sigma^{ad}_{O_{1s}} n^{ad}_{O} \lambda^{ad}_{O_{1s}},$$

and if the $d_{ad}(1/\lambda^{ad}_{Si_{2p}} - 1/\lambda^{ad}_{O_{1s}})$ value is assumed to be very small, then

$$\Delta \simeq \frac{K}{I^{oxide}_{Si_{2p}}} \left[\exp\left(\frac{d_{ad}}{\lambda^{ad}_{Si_{2p}}}\right) - 1 \right] + \frac{I^{oxide}_{O_{1s}} - K}{I^{oxide}_{Si_{2p}}} \left(\frac{1}{\lambda^{ad}_{Si_{2p}}} - \frac{1}{\lambda^{ad}_{O_{1s}}}\right) d_{ad}. \tag{17}$$

As shown in fig. 4, the $I^{oxide}_{O_{1s}}/I^{oxide}_{Si_{2p}}$ values scarcely changed by heating to 300°C for 1 h. Therefore,

$$\delta\Delta = \left[\frac{K}{\lambda^{ad}_{Si_{2p}} I^{oxide}_{Si_{2p}}} \exp\left(\frac{d_{ad}}{\lambda^{ad}_{Si_{2p}}}\right) + \frac{I^{oxide}_{O_{1s}} - K}{I^{oxide}_{Si_{2p}}} \left(\frac{1}{\lambda^{ad}_{Si_{2p}}} - \frac{1}{\lambda^{ad}_{O_{1s}}}\right) \right] \delta d_{ad},$$

where δd_{ad} was not zero, because the intensity of C_{1s} emitted from the adsorption layer decreased by 40--60% upon heating at 300°C for 1 h.

Then, eq. (17) can be rewritten as

$$\Delta = \frac{K}{I^{oxide}_{Si_{2p}}} \left[\exp\left(\frac{d_{ad}}{\lambda^{ad}_{Si_{2p}}}\right) - 1 - \frac{d_{ad}}{\lambda^{ad}_{Si_{2p}}} \exp\left(\frac{d_{ad}}{\lambda^{ad}_{Si_{2p}}}\right) \right]. \tag{18}$$

Since d_{ad} can be considered to be much smaller than $\lambda^{ad}_{Si_{2p}}$,

$$\Delta = \frac{K}{I^{oxide}_{Si_{2p}}} \left[\left(1 + \frac{d_{ad}}{\lambda^{ad}_{Si_{2p}}}\right) \left(1 - \frac{d_{ad}}{\lambda^{ad}_{Si_{2p}}}\right) - 1 \right] \simeq 0, \tag{19}$$

and the effect of adsorption on the $I^{oxide}_{O_{1s}}/I^{oxide}_{Si_{2p}}$ ratio is negligible, although d_{ad} is not zero [Δ does not contain terms proportional to $(d_{ad}/\lambda^{ad}_{Si_{2p}})^1$ but only contains terms proportional to $(d_{ad}/\lambda^{ad}_{Si_{2p}})^2$ or of higher order].

In fig. 4, experimental data deviated from the solid curve and the degree of

deviation was much larger for thinner oxide films. This deviation shows that the composition differs from stoichiometric SiO_2 for very thin oxide films.

Next, the composition of the oxide film was determined from the relationship between the experimental data, $(I^{oxide}_{O_{1s}}/I^{oxide}_{Si_{2p}})_{exp}$, and the calculated value for stoichiometric SiO_2, $(I^{SiO_2}_{O_{1s}}/I^{SiO_2}_{Si_{2p}})_{calc}$, in fig. 4. When an oxide film is represented as SiO_x, the apparent composition can be also written as

$$\frac{n^{oxide}_{O}}{n^{oxide}_{Si}} = x = 2\left(\frac{I^{oxide}_{O_{1s}}}{I^{oxide}_{Si_{2p}}}\right)_{exp}\Bigg/\left(\frac{I^{SiO_2}_{O_{1s}}}{I^{SiO_2}_{Si_{2p}}}\right)_{calc}. \tag{20}$$

The composition obtained from eq. (20) is not the actual composition but "the apparent composition". In other words, this is the composition obtained from the photoelectron intensity ratio [see eq. (20)] by assuming a constant composition in the oxide film. And if a concentration gradient exists in the oxide film, the composition obtained by ESCA represents only the apparent composition. Moreover, this apparent composition is also not average composition, because the photoelectron intensity from the surface region is larger than that from the substrate region. The relationship between the apparent composition and the oxide film thickness is shown in fig. 5. It is clear that the apparent composition of the very thin oxide is non-stoichiometric and Si-rich.

The composition obtained is only an apparent one and the actual concentration profile will be discussed in section 3.5 based on the relationship between the appar-

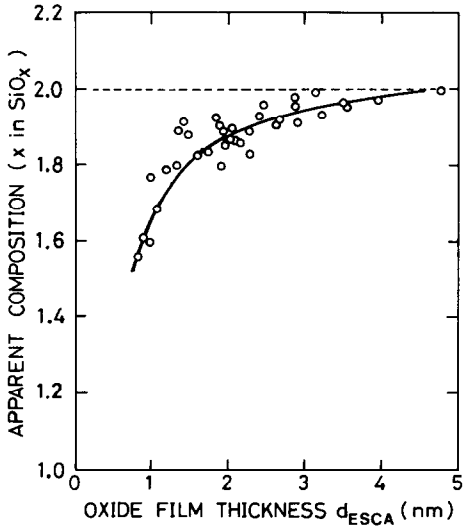

Fig. 5. Relationship between the apparent composition and d_{ESCA}.

ent composition and the oxide film thickness, after a discussion of the chemical state of the oxide films in the next section.

3.4. Chemical state of Si atoms in oxide film

Careful observations of Si_{2p} spectra were carried out to clarify the phase existing at the Si–SiO_2 interface. Examples of Si_{2p} spectra are shown in fig. 6. Si_{2p} can be separated into three peaks, two of which correspond to oxidized Si and one to Si crystal. The Si_{2p}^{Si} peak shape (which was asymmetric) assumed to be similar to that of a freshly etched Si crystal, as mentioned previously. The $Si_{2p}^{SiO_2}$ peak shape was assumed to be symmetrical because its shape for a very thick oxide film (200 nm) was symmetrical. The peak lowest in kinetic energy is associated with $Si_{2p}^{SiO_2}$, the one in the middle with an unidentified phase, $Si_{2p}^{SiO_y}$ (probably Si_{2p}^{SiO}), and the one highest in kinetic energy with Si_{2p}^{Si}.

The position of $Si_{2p}^{SiO_2}$ shifts to a lower kinetic energy as the thickness increases

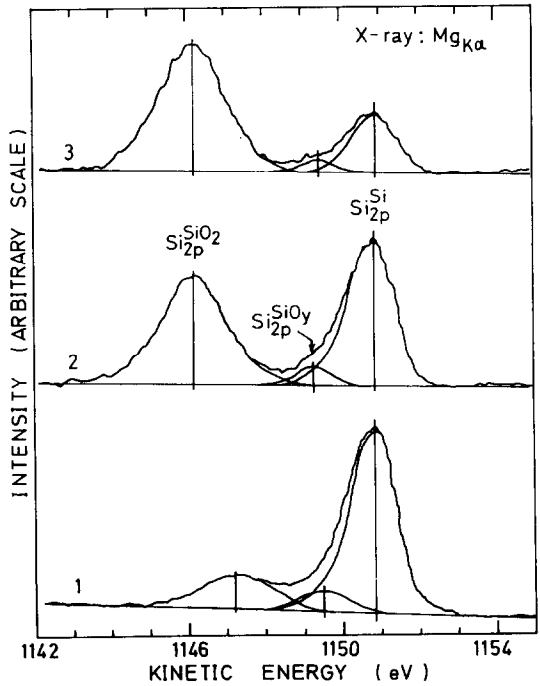

Fig. 6. Typical examples of Si_{2p} photoelectron spectra. The Si_{2p} spectrum is made up of three peaks, namely, $Si_{2p}^{SiO_2}$, $Si_{2p}^{SiO_y}$ and Si_{2p}^{Si}. Peak separation was carried out by assuming the Si_{2p}^{Si} peak shape to be similar to that of a freshly etched Si crystal and the $Si_{2p}^{SiO_2}$ peak shape to be symmetrical. (1) d_{ESCA} = 0.91 nm; (2) d_{ESCA} = 2.20 nm; (3) d_{ESCA} = 3.95 nm.

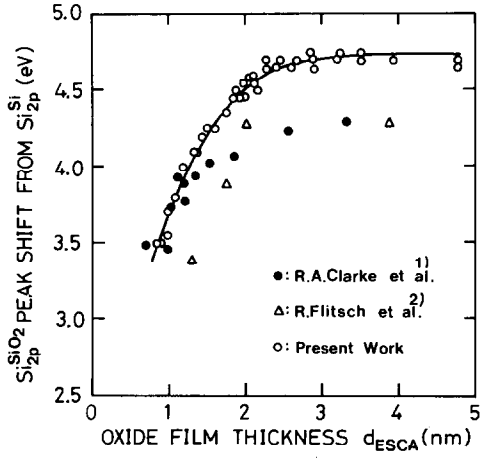

Fig. 7. Relationship between the position shift of the $Si_{2p}^{SiO_2}$ peak from the Si_{2p}^{Si} peak and the oxide film thickness.

(fig. 7). Similar results were reported by Flitsch et al. [2,5] and Clarke et al. [1], and they stated that this behavior represents the change of chemical state for extremely thin oxide films.

However, the result of our other experiment, which will be reported elsewhere [31–33], shows that the $Si_{2p}^{SiO_2}$ and O_{1s}^{oxide} peak positions move for different X-ray exposure times for the same sample, and the peak position returns to the original position when X-ray exposure is terminated. (The results are reproducible for the same sample.) Furthermore, these peak positions depend on X-ray intensities. These facts suggest that the chemical shift of a thin oxide film, which is an insulator, as measured by ESCA is determined not only by the chemical state but also by the X-ray-induced electric charges in the oxide films. In addition to this, figs. 1 and 8 show that the shifts of the O_{1s}^{oxide} peaks are the same as those of $Si_{2p}^{SiO_2}$ peaks (fig. 8). This fact also supports that there is indeed charging. This result contradicts that of Raider et al. [5], in which they say that "the experimentally obtained oxide film O_{1s} binding energies, although scattered, appear unchanged both within the transition region and the stoichiometric oxide film". The reasons for the above difference are not known. However, it should be pointed out that all our photoelectron spectra, Si_{2p} and O_{1s}, were measured after 30–60 min X-ray exposure (when the peak positions became constant). The peak positions thus obtained were not scattered (reproducible to within ±0.15 eV for any thickness and to within ±0.1 eV for the same sample), and showed a definite dependence on the oxide thickness. Furthermore, the concentration analysis (in section 3.5) shows that the oxide film is composed mainly of stoichiometric SiO_2. This result roughly agrees with Grunthaner's result [4] and with that of Raider [5], where the thickness of the transition layer was less than 1 nm thick. Consequently, it is believed that the peak

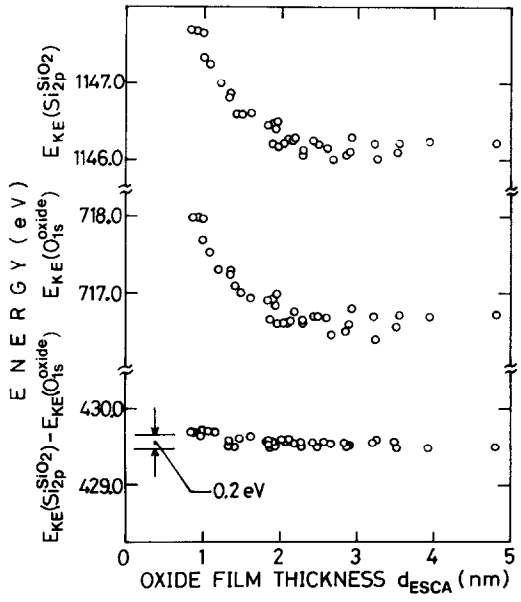

Fig. 8. Dependence of the oxide film thickness d_{ESCA} on the $Si_{2p}^{SiO_2}$ peak position, the O_{1s}^{oxide} peak position in kinetic energy and the balance of the peak position from $Si_{2p}^{SiO_2}$ to O_{1s}^{oxide}.

lowest in kinetic energy is due to stoichiometric SiO_2, and the peak position changes were caused by electric charging.

The chemical state of SiO_y will now be discussed. The value of y in SiO_y was roughly estimated to be 0.6–0.9 * because the peak positions of $Si_{2p}^{SiO_y}$ were 1.3–1.5 eV lower and those of $Si_{2p}^{SiO_2}$ were 3.5–4.7 eV lower in kinetic energy than that of Si_{2p}^{Si}. Moreover, the consideration of a charging effect should make the value of y greater than those just obtained. More detailed analyses of the composition and the chemical state of this phase will be discussed in the next section (3.5), where the SiO_y phase is identified as SiO.

The intensity of $Si_{2p}^{SiO_y}$ decreases in a manner similar to the intensity of the Si_{2p}^{Si} peak as the oxidation proceeds. The intensity ratios of $Si_{2p}^{SiO_y}$ to Si_{2p}^{Si} for various samples were between 0.10 to 0.15, and dependence of these ratios on the oxide film thickness was not observed. This shows that this phase is at about the same depth as Si, which makes it very likely that this phase is at the Si–SiO_2 interface,

* This value was determined from [34] $\Delta E = q\ (1/r - \alpha/R)$, where ΔE is the chemical shift, q is the number of electrons transferred, r is the mean radius of the valence shell, R is the average distance to which the charge is transferred when a chemical bond is established, and α is the Madelung constant. In this equation, it was assumed that $(1/r - \alpha/R)$ was constant for SiO_y and SiO_2.

and that its thickness is roughly constant. Its thickness was found to be 0.3 ± 0.1 nm by assuming that this phase is SiO and that $\lambda_{Si_{2p}}^{SiO} = \lambda_{Si_{2p}}^{SiO_2} = \lambda_{Si_{2p}}^{oxide}$, $\sigma_{Si_{2p}}^{SiO} = \sigma_{Si_{2p}}^{SiO_2} = \sigma_{Si_{2p}}^{Si}$ [29], and $\rho_{SiO} = 2.23$ Mg/m^3 [35] in eq. (21), which is rewritten as

$$d_{ESCA}^{SiO} = \frac{\lambda_{Si_{2p}}^{SiO}}{1.35} \ln\left(\frac{\rho_{Si} M_{SiO} \lambda_{Si_{2p}}^{Si} I_{Si_{2p}}^{SiO}}{\rho_{SiO} M_{Si} \lambda_{Si_{2p}}^{SiO} I_{Si_{2p}}^{Si}} + 1\right) = 2.59 \ln\left(0.932 \frac{I_{Si_{2p}}^{SiO}}{I_{Si_{2p}}^{Si}} + 1\right). \quad (21)$$

If this phase is more Si-rich than SiO, as implied by its peak position, its thickness is expected to be even smaller than 0.3 nm because M_{SiO_y} decreases for smaller y and $\lambda_{2p}^{SiO_y}$ is also expected to decrease for smaller y.

3.5. Concentration profile in the oxide film on Si

The concentration profile in the oxide film on Si was determined on the basis of the results of the apparent composition and chemical state analyses.

It was shown in the last section that there was a phase different from SiO_2 at the Si–SiO_2 interface. It was assumed in this section that a layer of SiO, thickness d_1, existed at the interface, and that the rest of the oxide film was assumed, for simplicity, to be SiO_2, with thickness $d_2 = d_{ESCA} - d_1$ (see fig. 9). Then the relationship between the apparent composition and d_{ESCA} can be obtained from eq. (14)

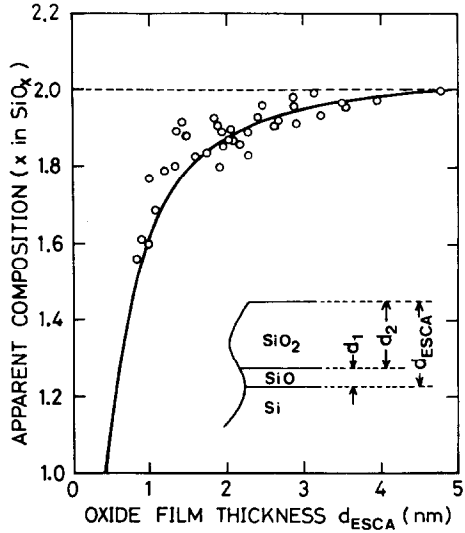

Fig. 9. Apparent composition calculated by assuming the concentration profile shown in the diagram. The solid curve represents the calculated relation for the case of $d_1^{Si} = 0.2$ nm, $d_1^{O} = 0$ nm and $d_2^{Si} = d_2^{O}$.

and $(I^{oxide}_{O_{1s}}/I^{oxide}_{Si_{2p}})_{calc}$, which can be written as

$$\left(\frac{I^{oxide}_{O_{1s}}}{I^{oxide}_{Si_{2p}}}\right)_{calc} = \frac{(I^{SiO}_{O_{1s}} + I^{SiO_2}_{O_{1s}}}{(I^{SiO}_{Si_{2p}} + I^{SiO_2}_{Si_{2p}})}$$

$$= \left\{\sigma^{SiO}_{O_{1s}} \frac{\rho_{SiO}}{M_{SiO}} \lambda^{SiO}_{O_{1s}} \left[1 - \exp\left(-\frac{1.35d^O_1}{\lambda^{SiO}_{O_{1s}}}\right)\right] \exp\left(-\frac{1.35d^O_2}{\lambda^{SiO_2}_{O_{1s}}}\right)\right.$$

$$\left. + \sigma^{SiO_2}_{O_{1s}} \frac{2\rho_{SiO_2}}{M_{SiO_2}} \lambda^{SiO_2}_{O_{1s}} \left[1 - \exp\left(-\frac{1.35d^O_2}{\lambda^{SiO_2}_{O_{1s}}}\right)\right]\right\}$$

$$\times \left\{\sigma^{SiO}_{Si_{2p}} \frac{\rho_{SiO}}{M_{SiO}} \lambda^{SiO}_{Si_{2p}} \left[1 - \exp\left(-\frac{1.35d^{Si}_1}{\lambda^{SiO}_{Si_{2p}}}\right)\right] \exp\left(-\frac{1.35d^{Si}_2}{\lambda^{SiO_2}_{Si_{2p}}}\right)\right.$$

$$\left. + \sigma^{SiO_2}_{Si_{2p}} \frac{\rho_{SiO_2}}{M_{SiO_2}} \lambda^{SiO_2}_{Si_{2p}} \left[1 - \exp\left(-\frac{1.35d^{Si}_2}{\lambda^{SiO_2}_{Si_{2p}}}\right)\right]\right\}^{-1} \quad (22)$$

where different thicknesses are used for calculating $I^{oxide}_{O_{1s}}$ and $I^{oxide}_{Si_{2p}}$, so that $d^{Si}_{ESCA} = d^{Si}_1 + d^{Si}_2$ and $d^{O}_{ESCA} = d^{O}_1 + d^{O}_2$. In section 3.2, it was shown that d^{Si}_{ESCA} was not the same as d^{O}_{ESCA}, and that the difference $(d^{Si}_{ESCA} - d^{O}_{ESCA})$ was 0.24 nm (equal to $C' - C$). This value is roughly equal to d_1 obtained from $Si^{SiO}_{2p}y$ $(=d^{Si}_1)$ in section 3.4. This means that d^{O}_{ESCA} is nearly equal to d^{Si}_2 (obtained from the $Si^{SiO_2}_{2p}$ intensity). If it is assumed that $d^{Si}_2 = d^{O}_2$, d^{O}_1 is nearly zero. Then, the values of the apparent composition for various oxide thicknesses were calculated by assigning several different values to d^{Si}_1. It was assumed here that $d^{Si}_2 = d^{O}_2$, $d^{O}_1 = 0$, $\sigma^{SiO_2}_{O_{1s}} = \sigma^{SiO}_{O_{1s}}$, $\sigma^{SiO_2}_{Si_{2p}} = \sigma^{SiO}_{Si_{2p}}$ [29], $\lambda^{SiO_2}_{O_{1s}} = \lambda^{SiO}_{O_{1s}}$ and $\lambda^{SiO_2}_{Si_{2p}} = \lambda^{SiO}_{Si_{2p}}$. the best fit with the experimental data was obtained for $d^{Si}_1 = 0.2$ nm, as shown in fig. 9. This result is in rough agreement with the result of section 3.4, i.e. that SiO_y is about 0.2 nm thick.

The assumed concentration profile of Si atoms in the oxide film which agreed best with the experimental results is shown in fig. 10. The concentration for $d > 0.6$ nm would remain essentially the same ($x = 2$) even if the concentration was allowed to change continuously, instead of abruptly, as shown.

The chemical state of SiO_y is now discussed again. The concentration profile just obtained shows that the oxide film on Si is SiO_2 down to at least 0.6 nm thick. Then, it is believed that the change in $Si^{SiO_2}_{2p}$ peak position in fig. 7 is caused by charging rather than by chemical state change. Therefore, the true chemical shift of SiO_2 can be determined by extrapolation to zero SiO_2 thickness, where no charging effect is to be expected, and this value is obtained as 2.5–3.0 eV from the extrapolation of the curve to $d_2 = 0$ (equal to $d^{Si}_{ESCA} = 0.3$ nm) in fig. 7. Furthermore, this value just obtained is also supported by our other experiment in which the true chemical shifts of the $Si^{SiO_2}_{2p}$ for 1, 3 and 4 nm thick oxide films were obtained as 3.0 ± 0.2 eV from the X-ray intensity dependence of the $Si^{SiO_2}_{2p}$ peak position

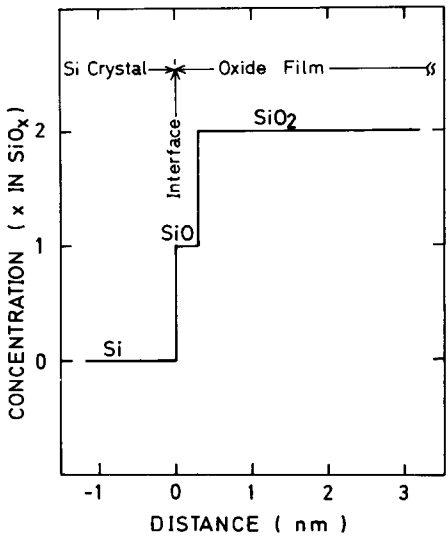

Fig. 10. Concentration profile in the oxide film on Si.

[31–33]. On the other hand, the chemical shift of SiO_y was 1.3–1.5 eV as shown in fig. 6. Thus, the chemical shift of SiO_y is about one half of that of SiO_2, so that $y = 0.9$–1.0 and SiO_y phase is probably SiO.

Then, it can be summarized that the value d_1^{Si} obtained from the composition analysis is 0.3 nm if it is assumed that d_1^O is zero, and that the value d_1^{Si} obtained from the Si_{2p}^{SiO} photoelectron intensity analysis is 0.2 nm. These two results are in rough agreement. However, these results were obtained by using the λ values which were determined under the assumption that the oxide film was of uniform composition. The result just obtained shows that the oxide film is actually composed of SiO and SiO_2. The λ values were therefore re-evaluated for the actual case where the oxide film was composed of SiO and SiO_2 (see Appendix). From this re-evaluation, the following results were obtained, i.e., d_1^O was also zero and d_1^{Si} was 0.31 nm (fig. 11). The results just obtained were almost in agreement with the results previously obtained, and these can explain the results of the chemical state, and the compositional and escape depth analyses without discrepancy.

Physically speaking, this SiO is considered to be the first monolayer (the atomic diameter of Si is 0.24 nm) of Si in contact with SiO_2, the chemical state of the Si atoms in the transition layer is Si^{2+}, and no O atoms are contained in the transition layer (d_1^{Si}). This Si^{2+} layer is called "SiO" in this paper although it does not contain any O atoms. It might seem strange, but it is not so for the following reasons: (1) The thickness of the "SiO" was defined from the ESCA peak intensities of the Si_{2p} and O_{1s}. (2) The O in the SiO and SiO_2 cannot be distinguished by ESCA (both O^{2-}), and all O atoms were included in the SiO_2. (3) No Si^{2+} is present in the SiO_2 (d_2^{Si} or d_2^O) (see fig. 11).

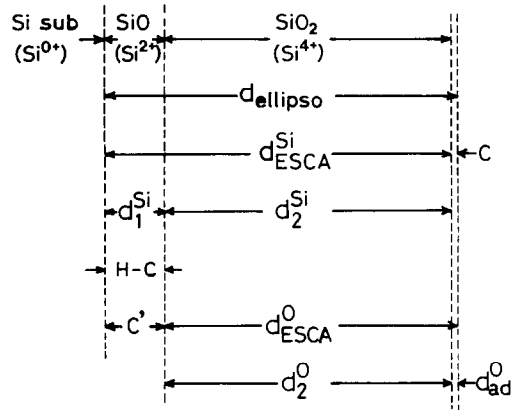

Fig. 11. Schematic relations among $d_{ellipso}$, d^{Si}_{ESCA}, d^{O}_{ESCA}, d^{Si}_{1}, d^{Si}_{2}, d^{O}_{2}, H, C and C'.

4. Conclusion

This study was carried out to find the concentration profile in the thermal oxide film on Si near the Si–SiO_2 interface by using ESCA and ellipsometry. The results are as follows:

(1) The values of the mean escape depths used for the present analysis were 3.49 and 1.68 nm for $\lambda^{oxide}_{Si_{2p}}$ and $\lambda^{oxide}_{O_{1s}}$, respectively.

(2) Although the composition of oxide film as a whole appeared to be Si-rich for thicknesses less than about 3 nm, the oxide film was probably composed mostly of stoichiometric SiO_2 with a very thin (0.3 nm) layer of SiO at the Si–SiO_2 interface.

Acknowledgements

The authors would like to express their gratitude to Drs. K. Sato, A. Fukuhara, Y. Katayama, Y. Itoh, Messrs. M. Maki, K. Usami and Y. Takehana for many helpful suggestions they made during the course of this study.

Appendix

In this paper, it was found that the oxide film was composed of SiO_2 and SiO. In section 3.2, the mean escape depth values of the photoelectrons were determined by assuming the composition to be constant in the oxide film, and composition analysis was carried out by using these values.

In this section, the mean escape depth values were re-evaluated for the actual

case where the oxide film is composed of SiO_2 and SiO. Furthermore, the meaning of the value, C, was clarified.

The intensity ratio, $I^{oxide}_{Si_{2p}}/I^{Si}_{Si_{2p}}$, can be rewritten as

$$I^{oxide}_{Si_{2p}}/I^{Si}_{Si_{2p}} = (I^{SiO}_{Si_{2p}} + I^{SiO_2}_{Si_{2p}})/I^{Si}_{Si_{2p}}$$

$$= \frac{n^{SiO}_{Si}\lambda^{SiO}_{Si_{2p}}[1 - \exp(-1.35d^{Si}_1/\lambda^{SiO}_{Si_{2p}}]}{n^{Si}_{Si}\lambda^{Si}_{Si_{2p}}} + \frac{n^{SiO_2}_{Si}\lambda^{SiO_2}_{Si_{2p}}[\exp(1.35d^{Si}_2/\lambda^{SiO_2}_{Si_{2p}}) - 1]}{n^{Si}_{Si}\lambda^{Si}_{Si_{2p}}\exp(-1.35d^{Si}_1/\lambda^{SiO}_{Si_{2p}})}$$

$$= E + F\{\exp[G(d_{ellipso} - H)] - 1\}, \quad (23)$$

where d^{Si}_1 and d^{Si}_2 are the thicknesses of SiO and SiO_2, respectively. The values obtained were $E = 0.100 \pm 0.001$, $F = 0.879 \pm 0.019$, $G = 0.387 \pm 0.001$ nm^{-1} and $H = 0.35 \pm 0.01$ nm by the method of least squares with the use of the data in fig. 2. Then, $\lambda^{SiO_2}_{Si_{2p}}$ was obtained as 3.49 ± 0.01 nm which turned out to be the same as $\lambda^{oxide}_{Si_{2p}}$. The $\lambda^{Si}_{Si_{2p}}$ value was determined to be 2.3 ± 0.3 nm. Though the $\lambda^{Si}_{Si_{2p}}$ value just obtained is somewhat larger than that obtained in section 3.2, it seems certain that λ considerably depends on the material in which the electrons pass. On the other hand, the $\lambda^{SiO}_{Si_{2p}}$ value could not be determined exactly, and the $\lambda^{SiO}_{Si_{2p}}$ value obtained was 0.7–3.4 nm.

Next, the relations among $d_{ellipso}$, d^{Si}_{ESCA}, d^{O}_{ESCA}, d^{Si}_1, d^{Si}_2, d^{O}_1, d^{O}_2, H, C in eq. (8) and C' in eq. (12) were considered. The value of $d_{ellipso}$ was equal to $(d^{Si}_{ESCA} + C)$ and to $(d^{Si}_1 + d^{Si}_2 + C)$. Then, $(H - C)$ came to be equal to d^{Si}_1 and this value was 0.31 ± 0.03 nm. The value of $d_{ellipso}$ was also equal to $(d^{O}_{ESCA} + C')$ where C' was 0.28 ± 0.01 nm. This C' value was almost equal to d^{Si}_1 and this means that d^{O}_1 is zero. The value of $(H - C')$ was 0.07 ± 0.02 nm, and this value was roughly equal to C (0.04 ± 0.02 nm). These C and $(H - C')$ values are interpreted as the thickness of the adsorption layer, and this means that d^{O}_{ESCA} contained d^{O}_{ad} ($d^{O}_{ESCA} = d^{O}_2 + d^{O}_{ad}$ and $d^{O}_{ad} \ll d^{O}_2$). The schematic relations just obtained are shown in fig. 11.

Next, the $\lambda^{SiO_2}_{O_{1s}}$ value was considered. The slope of the line in fig. 3 which is $1.35/\lambda^{oxide}_{O_{1s}}$, is equal to $1.35/\lambda^{SiO_2}_{O_{1s}}$, because this slope is only determined by the relationship between $[1 - I_{O_{1s}}/I_{O_{1s}}(d = \infty)]$ and $d_{ellipso}$ (not d^{O}_{ESCA} or d^{O}_2). Therefore, the $\lambda^{SiO_2}_{O_{1s}}$ value obtained was 1.68 ± 0.03 nm which was equal to the $\lambda^{oxide}_{O_{1s}}$ value.

Since the values of $\lambda^{SiO_2}_{Si_{2p}}$ and $\lambda^{SiO_2}_{O_{1s}}$ are equal to $\lambda^{oxide}_{Si_{2p}}$ and $\lambda^{oxide}_{O_{1s}}$, respectively, the composition analysis in section 3.3 is valid.

References

[1] R.A. Clarke, R.L. Tapping, M.A. Hopper and L. Young, J. Electrochem. Soc. 122 (1975) 1347.

[2] R. Flitsch and S.I. Raider, J. Vacuum Sci. Technol. 12 (1975) 305.

[3] S.I. Raider and R. Flitsch, J. Vacuum Sci. Technol. 13 (1976) 58.
[4] F.J. Grunthaner and J. Maserjian, IEEE Trans. Nucl. Sci. NS-24 (1977) 2108.
[5] S.I. Raider and R. Flitsch, IBM J. Res. Develop. 22 (1978) 294.
[6] J.S. Johannessen and W.E. Spicer, J. Vacuum Sci. Technol. 13 (1976) 849.
[7] J.S. Johannessen and W.E. Spicer, J. Appl. Phys. 47 (1976) 3028.
[8] C.C. Chang and D.M. Boulin, Surface Sci. 69 (1977) 385.
[9] A. Benninghoven and S. Storp, Appl. Phys. Letters 22 (1973) 170.
[10] A. Benninghoven, Surface Sci. 35 (1973) 427.
[11] T.W. Sigmon, W.K. Chu, E. Lugujjo and J.W. Mayer, Appl. Phys. Letters 24 (1974) 105.
[12] H.R. Philipp, J. Phys. Chem. Solids 32 (1971) 1935.
[13] H.R. Philipp, J. Appl. Phys. 43 (1974) 2835.
[14] J. Blanc, C.J. Buiocchi, M.S. Abrahams and W.E. Ham, Appl. Phys. Letters 30 (1977) 120.
[15] O.L. Krivanek, T.T. Sheng and D.C. Tsui, Appl. Phys. Letters 32 (1978) 437.
[16] M. Klasson, A. Berndtsson, J. Hedman, R. Nilsson, R. Nyholm and C. Nordling, J. Electron Spectrosc. Related Phenomena 3 (1974) 427.
[17] D.R. Penn, J. Electron Spectrosc. Related Phenomena 9 (1976) 29.
[18] D.R. Penn, Phys. Rev. B13 (1976) 5248.
[19] F.J. Grunthaner, NBS Special Publication 400-23 (1976) 151.
[20] G. Leonhardt and H.J. Bilz, Kristall Tech. 10 (1975) K35.
[21] Y.J. van der Meulen, J. Electrochem. Soc. 119 (1972) 530.
[22] T. Smith and A.J. Carlen, J. Appl. Phys. 43 (1972) 2455.
[23] Y. Kamigaki and Y. Itoh, J. Appl. Phys. 48 (1977) 2891.
[24] F.L. McCrackin and J.P. Coison, NBS Tech. Note 242 (1964).
[25] T.A. Carlson, J. Electron Spectrosc. Related Phenomena 1 (1972/1973) 161.
[26] H. Edagawa, Y. Morita, S. Maekawa and Y. Inoishi, Japan, J. Appl. Phys. 2 (1963) 765.
[27] B.E. Deal, J. Electrochem. Soc. 110 (1963) 527.
[28] B.E. Deal, J. Electrochem. Soc. 115 (1968) 300.
[29] V.I. Nefedov, N.P. Sergushin, I.M. Band and M.B. Trzhanskovskaya, J. Electron Spectrosc. Related Phenomena 2 (1973) 383.
[30] J.H. Scofield, J. Electron Spectrosc. Related Phenomena 8 (1976) 129.
[31] S. Iwata and A. Ishizaka, in: Abstr. 83rd Meeting of the Japan Institute of Metals (1978) p. 58.
[32] S. Iwata and A. Ishizaka, J. Japan. Inst. Metals 42 (1978) 1020.
[33] S. Iwata and A. Ishizaka, J. Japan, Inst. Metals 43 (1979) 380, 389.
[34] K. Siegbahn, C. Nordling, A. Fahlman, R. Nordberg, K. Hamrin, J. Hedman, G. Johansson, T. Bergmark, S.E. Karlsson, I. Lindgren and B. Lindberg, ESCA–Atomic, Molecular and Solid State Structure Studied by Means of Electron Spectroscopy, Nova Acta Reg. Soc. Sci. Upsaliensis, Ser. IV, 20 (1967) 81.
[35] W.A. Pliskin and H.S. Lehman, J. Electrochem. Soc. 112 (1965) 1013.